Bioorganic & Medicinal Chemistry 20 (2012) 510–520

Contents lists available at SciVerse ScienceDirect

Bioorganic & Medicinal Chemistry

journal homepage: www.elsevier.com/locate/bmc

Optimizing thiadiazole analogues of resveratrol versus three chemopreventive targets

Abdelrahman S. Mayhoub [a,†], Laura Marler [b], Tamara P. Kondratyuk [b], Eun-Jung Park [b], John M. Pezzuto [b], Mark Cushman [a,*]

[a] Department of Medicinal Chemistry and Molecular Pharmacology, College of Pharmacy and the Purdue Center for Cancer Research, Purdue University, West Lafayette, IN 47907, USA
[b] College of Pharmacy, University of Hawaii at Hilo, Hilo, HI 96720, USA

ARTICLE INFO

Article history:
Received 11 June 2011
Revised 13 September 2011
Accepted 19 September 2011
Available online 25 September 2011

Keywords:
Thiadiazole
Cancer chemoprevention
Aromatase
QR1
NF-κB

ABSTRACT

Chemoprevention is an approach to decrease cancer morbidity and mortality through inhibition of carcinogenesis and prevention of disease progression. Although the *trans* stilbene derivative resveratrol has chemopreventive properties, its action is compromised by weak non-specific effects on many biological targets. Replacement of the stilbene ethylenic bridge of resveratrol with a 1,2,4-thiadiazole heterocycle and modification of the substituents on the two aromatic rings afforded potential chemopreventive agents with enhanced potencies and selectivities when evaluated as inhibitors of aromatase and NF-κB and inducers of quinone reductase 1 (QR1).

1. Introduction

Drugs that prevent disease from developing offer attractive alternatives to those used in treatment. The use of aspirin to prevent coronary heart diseases is a familiar example.[1] Tamoxifen[2] and fenasteride[3] are examples of drugs that have been employed as breast and prostate cancer chemopreventive agents, respectively.

The concept of cancer chemoprevention refers to delaying and/or preventing cancer development.[4] Cancer chemoprevention can theoretically be achieved by reducing the effects of carcinogens by inhibiting or down-regulating phase I enzymes such as aromatase and inducible nitric oxide synthase (iNOS) that are capable of generating carcinogenic species.[5,6] Aromatase, the key enzyme in endogenous estrogen production, is an established target in breast cancer chemotherapy.[7] Since aromatase transcription is mediated by a known cancer-promoting kinase IkB kinase β (IKKβ), its inhibitors are also considered to be chemopreventive agents.[8] iNOS is involved in the immune response by catalyzing a high level of NO production.[9] However, excessive and persistent expression of iNOS and production of NO can contribute to pathological conditions including inflammatory diseases as well as cancer. In fact, the overexpression of iNOS has been reported in many cancer types.[10] On the other hand, chemoprevention could also be achieved by activating cytoprotective enzymes such as quinone reductase 1 (QR1).[11] An additional target for development of cancer chemopreventive agents is NF-κB, which regulates the expression of anti-apoptotic genes and is up-regulated in cancer cells due to gene mutation or secretion of NF-κB activating factors.[12,13] Therefore, down-regulation of NF-κB hinders cancer progression and cell differentiation via apoptosis activation. In addition, NF-κB plays a pivotal role in immune system regulation.[14] It can be activated by variable stimuli including interleukin 1β,[15] oxidants,[16] and some small molecules such as cocaine.[17] The NF-κB pathway is also involved in HIV-1 replication and pathogenesis.[18] Based on our understanding of these various biological pathways, cancer chemoprevention could be achieved by selectively targeting any of the proteins involved.

Grapes have been reported to reduce the risk of certain types of cancer.[19] Grapes contain resveratrol,[20] a naturally occurring *trans* stilbene with anticancer[21] and cancer chemopreventive potential.[22,23] However, resveratrol lacks potency and specificity, and is

Abbreviations: ARE, antioxidant response element; BBO, multinuclear broadband observe; CD, concentration to double QR1 activity; DMEM, Dulbecco's Modified Eagle Medium; DRE, dioxin response element; IC_{50}, sample concentration which causes 50% inhibition; DPPH, 2,2-diphenyl-1-picrylhydrazyl; iNOS, inducible nitric oxide synthase; IR, QR1 induction ratio; LPS, lipopolysaccharide; NF-κB, nuclear factor kappa-light-chain-enhancer of activated B cells; Nrf2, nuclear factor erythroid 2-related factor 2; QNP, quattro nucleus probe; QR1, quinone reductase 1; TSO, *trans*-stilbene oxide; SRB, sulforhodamine B.

* Corresponding author. Tel.: +1 765 494 1465; fax: +1 765 494 6790.
E-mail address: cushman@purdue.edu (M. Cushman).
† On leave from Al-Azhar University, College of Pharmacy, Cairo, Egypt.

0968-0896/$ - see front matter © 2011 Elsevier Ltd. All rights reserved.
doi:10.1016/j.bmc.2011.09.031

converted rapidly into inactive metabolites.[8,24] Resveratrol's main disadvantage in chemoprevention is a poor pharmacokinetic profile due to the presence of free hydroxyl groups that are conjugated in vivo. Methylated analogues of resveratrol such as DMU-212[25] and trimethoxystilbene[26] have been used as chemopreventative agents that show enhanced potency due to tubulin binding and favorable pharmacokinetics. There is therefore interest in design and synthesis of resveratrol analogues with enhanced potencies, selectivities, and metabolic stabilities.

Resveratrol target specificity versus aromatase and quinone reductase 2 (QR2) has been improved by varying the substituents on the two phenyl rings.[27] Replacement of the alkene linker with heterocyclic systems is a complementary strategy that has been used to enhance the antitumor efficacy of the *cis* stilbene derivative combretastatin A-4.[28] In this report, both strategies have been combined. First, the *trans* stilbene ethylenic bridge of the resveratrol scaffold was replaced with five-membered heterocycles. Replacement of the *trans* stilbene ethylenic bridge with a 1,2-diphenyl heterocyclic system would change the geometric configuration of the two peripheral rings to resemble a *cis* stilbene (Fig. 1). To keep the geometry of these two phenyl rings relatively unchanged and close to that of the *trans* stilbene template, the phenyl rings were attached on the 1 and 3 positions of a five-membered heterocycle (Fig. 1). Based on this design, it was hypothesized that 1,3-diaryl five-membered heterocycles would retain the chemopreventive properties of the *trans* stilbene nucleus. This hypothesis has been tested, a lead compound was obtained, and then a series of analogues with different substituents were prepared. In order to address the chemopreventive target specificity, all of the compounds have been evaluated against a number of enzymes that are involved in chemopreventive pathways such as aromatase, NF-κB, iNOS, and QR1. Moreover, the direct antiproliferative effects of the compounds were evaluated in the estrogen receptor-positive breast cancer cell line MCF-7 and their antioxidant capacities were evaluated using a DPPH assay.

trans-Resveratrol was used as a reference compound in this study. In addition, its *cis* and double bond-reduced analogues were also tested to investigate whether the constrained *trans* geometry of the two aromatic rings on the alkene are necessary for biological activity in each case.

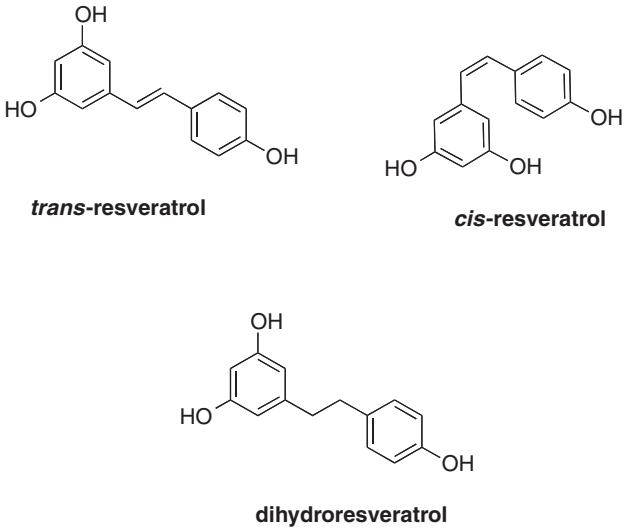

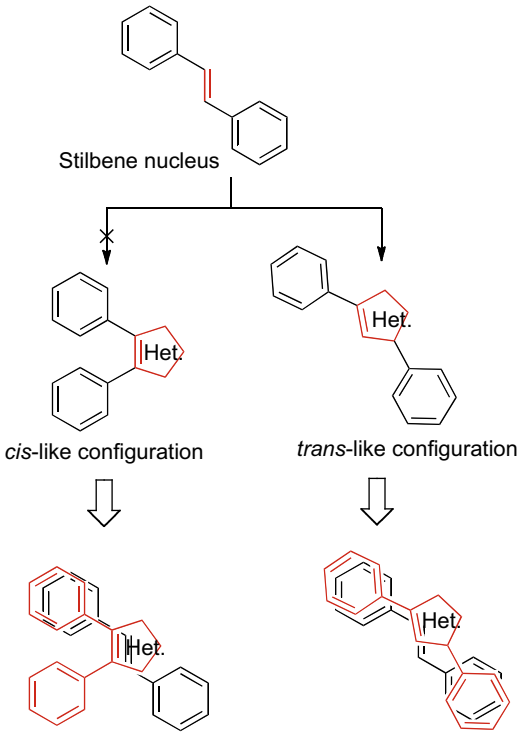

Figure 1. Design of 1,3-diaryl five-membered heterocycles from the stilbene template.

2. Results and discussion

2.1. Chemistry

Methyl bromocyanoacetate (**1**), prepared by bromination of commercially available methyl cyanoacetate with *N*-bromosuccinimide (NBS), was allowed to react with a set of thioamides **2a-ii** in absolute methanol at room temperature (Scheme 1). Non-commercially available thioamides **2ff**, **2gg**, **2hh**, and **2ii** were prepared from the reactions of their corresponding amides with Lawesson's reagent in dry THF.

The formation of the thiadiazole ring was confirmed by NMR and mass spectral data. For example, the ^{13}C NMR spectra of all of the 1,2,4-thiadiazoles **3a–ii** showed two distinct downfield quaternary carbon signals at about δ 182 and 175 ppm corresponding to the thiadiazole-C3 and -C5 carbons, respectively. The non-equivalence of these two carbons eliminates the corresponding 1,3,4-thiadiazole structure.

The diphenols **3jj** and **3kk** were prepared from their methoxy analogues **3g** and **3ii** by treatment with hydrogen bromide in glacial acetic acid at reflux temperature for 8 h (Scheme 2).

Catalytic hydrogenation of the dinitro derivative **3ff** afforded the corresponding diamino derivative **3ll** (Scheme 3).

2.2. Biological results

A preliminary study was conducted to test the hypothesis that 1,3-diaryl five-membered heterocycles can retain the chemopreventive properties of the stilbene nucleus. The stilbene analogue **3a** with a thiadiazole system at the position of the stilbene double bond was synthesized and tested for its potential chemopreventive activity. Interestingly, compound **3a** showed moderate to weak activity against aromatase and NF-κB, and a good induction ratio with QR1. Based on these initial results, it could be concluded that

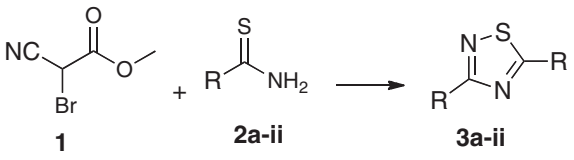

a, R = C_6H_5
b, R = 3-pyridyl
c, R = 4-pyridyl
d, R = 4-ClC_6H_5
e, R = 4-FC_6H_5
f, R = 4-BrC_6H_4
g, R = 4-$CH_3OC_6H_4$
h, R = 2-BrC_6H_4
i, R = 2-ClC_6H_4
j, R = 4-$CF_3C_6H_4$
k, R = 4-*t*BuC_6H_4
l, R = 4-IC_6H_4
m, R = 3-IC_6H_4
n, R = 3-FC_6H_4
o, R = 2-FC_6H_4
p, R = 3-BrC_6H_4
q, R = 2,3-$Cl_2C_6H_3$
r, R = 4-Cl-*o*-toluyl
s, R = 3-$CH_3C_6H_4$
t, R = 2-$CF_3C_6H_4$
u, R = 2,5-$Cl_2C_6H_3$
v, R = 3,4-$Cl_2C_6H_3$
w, R = 3-Cl-*o*-toluyl
x, R = 4-$CH_3C_6H_4$
y, R = 2-naphthyl
z, R = 4-*n*-BuC_6H_4
aa, R = 5-Cl-*o*-toluyl
bb, R = 4-Br-*o*-toluyl
cc, R = 2-IC_6H_4
dd, R = 2-Br-*p*-toluyl
ee, R = 2,4-$Cl_2C_6H_3$
ff, R = 4-$NO_2C_6H_4$
gg, R = 4-NCC_6H_4
hh, R = 3-NCC_6H_4
ii, R = 3-$CH_3OC_6H_4$

Scheme 1. Reagent and conditions: (a) Methanol, 23 °C, 1 min, 10–100%.

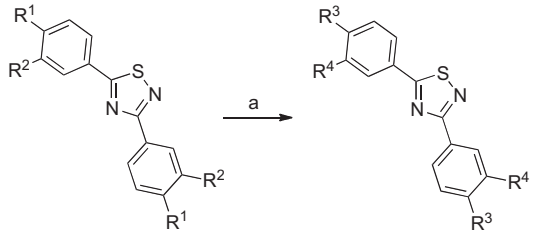

3g; R^1= OCH_3, R^2= H
3ii; R^1= H, R^2= OCH_3

3jj; R^3= OH, R^4= H
3kk; R^3= H, R^4= OH

[a]Reagents and conditions: (a) HBr, glacial acetic acid, heat to reflux for 8 h, 33-40%.

Scheme 2. Reagents and conditions: (a) HBr, glacial acetic acid, heat to reflux for 8 h, 33–40%.

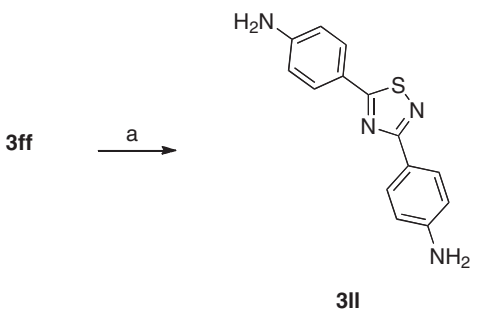

Scheme 3. Reagents and conditions: (a) H_2/Pd, methanol, 23 °C, 24 h, 40%.

the 3,5-diaryl-1,2,4-thiadiazole scaffold retains some of the chemopreventive activities of resveratrol.

Next, to increase the selectivity towards aromatase, a structure-based drug design approach was conducted using the available enzyme crystal structure.[29] The existing SAR data of the stilbene series on aromatase could not be directly applied here because the two peripheral rings of the stilbene and 3,5-disubstituted-1,2,4-thiadiazole systems do not overlap precisely, and the bridge provided by the heterocyclic system is slightly longer than an ethylenic bridge.

Compound **3a** was docked into the active pocket of aromatase (PDB ID 3eqm) using GOLD software.[30] The initial expectation was that the mild activity of the lead compound **3a** could be due to the interaction between the thiazole and the heme iron. However, none of the top 10 poses showed such an interaction. Instead, the hypothetical binding mode of the lead compound **3a** with aromatase (Fig. 2) indicated that one of the phenyl rings lies over the heme iron and the other one is surrounded by the Met374 and Val373 residues without any interaction with the heme iron.

The model provided a rationale for synthesis of pyridyl analogues in which the nitrogen of one pyridine ring would coordinate with the heme iron of aromatase and the other pyridine nitrogen would hydrogen bond with the NH of Met374 (Fig. 3). The aromatase active site is known to be large and quiet flexible,[31] so it was very difficult to predict the best nitrogen positions from our simple computational model. Therefore, all of the possible 2-, 3- and 4-pyridyl derivatives were taken into consideration. Both 3-pyridyl and 4-pyridyl derivatives **3b** and **3c** were synthesized successfully; however, the 2-pyridyl analogue could not be synthesized and it has never been reported. The 3-pyridyl analogue **3b** was found to be greater than 250 times more potent than the lead compound **3a** as an aromatase inhibitor and it displayed an IC_{50} of 0.2 μM (Table 1). Moving the nitrogen atom to position-4 (compound **3c**) partially suppressed the aromatase inhibitory activity (IC_{50} 0.8 μM, Table 1). Compounds **3b** and **3c** displayed a high degree of structural specificity, being the only compounds in the series that were aromatase inhibitors with IC_{50} values less than 50 μM except of the diamino compound **3ll**, which had an IC_{50} of 26.5 μM. Both **3a** and **3b** had a high degree of selectivity for aromatase versus the other targets investigated.

Based on these results, it seems that 3,5-dipyridyl-1,2,4-thiadiazoles could serve as a new class of non-steroidal aromatase inhibitors. Non-steroidal aromatase inhibitors in general have superior therapeutic benefits compared with their steroidal counterparts.[32]

As discussed earlier, the unsubstituted thiadiazole **3a** exhibited some NF-κB inhibitory activity (IC_{50} 47 μM) plus a high QR1 induction ratio (IR 8.6). Although the crystal structure of NF-κB is available,[33] a structure-based design approach to optimize **3a** is not possible because the mechanism of inhibition is not known. Similarly, the mechanism of QR1 induction by **3a** is yet to be determined. Therefore, a large set of mono- and disubstituted thiadiazoles was prepared and both QR1 and NF-κB assays were conducted in order to eventually elucidate more extensive structure–activity relationships (SAR). The results are summarized in Table 3. In addition, the same set of compounds was tested in a number of other indicative chemoprevention assays including DPPH free radical quenching, inhibition of NO production, and antiproliferative activity in the MCF-7 breast cancer cell line to test for activity and selectivity. The results are listed in Table 3.

QR1 plays an important role in carcinogen deactivation.[34] The thiadiazoles reported here have proven to be very effective QR1 inducers, with 23 of the tested compounds increasing the QR1 activity by a factor of two or more (Table 2). The top thiadiazole QR1 inducers include the unsubstituted thiadiazole **3a** and the 2-halogen-substituted thiadiazoles such as **3h** and **3i**. The most potent QR1 inducer is the 2-fluoro derivative **3o** (Table 2), which displayed a QR1 induction ratio of 10.5. The more bulky

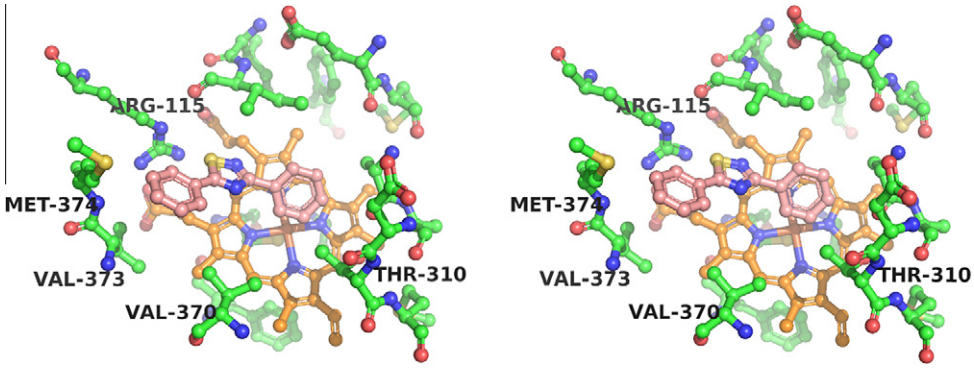

Figure 2. Hypothetical interaction between lead compound **3a**, and Met374, Arg115, Val370 and heme in the human aromatase active site. The heme backbone is colored orange. Many amino acid residues are deleted for the sake of clarity (PDB ID 3eqm). The stereoview is programmed for wall-eyed viewing.

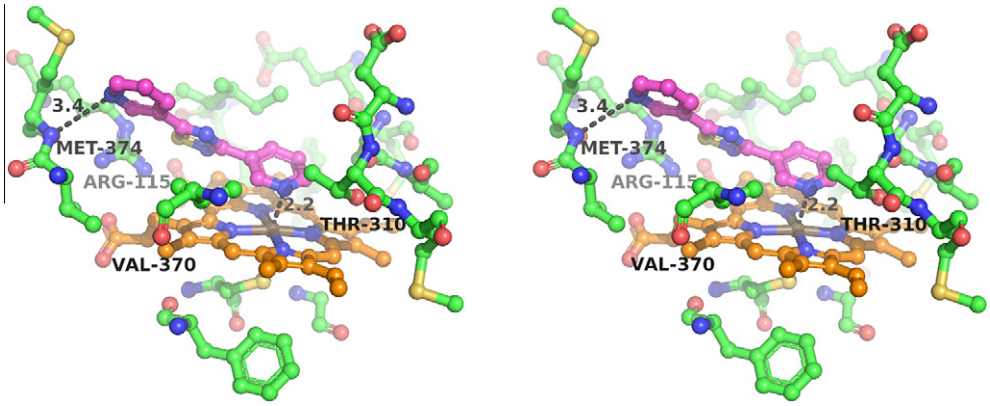

Figure 3. Hypothetical interaction between lead compound **3b** and Met374, Arg115 and heme in the human aromatase active site. Hydrogen bonds are represented by yellow dashed line. Many amino acid residues are deleted for the sake of clarity (PDB ID 3eqm). The stereoview is programmed for wall-eyed viewing.

Table 1
Inhibition of the human aromatase by thiadiazole **3** derivatives

Compound	Aromatase assay		Compound	Aromatase assay	
	% Max inhib[a]	IC_{50}[b] (μM)		% Max inhib[a]	IC_{50}[b] (μM)
3a	60.2 ± 2.8	>50	**3v**	23.0 ± 0.8	>50
3b	97.2 ± 1.4	0.2 ± 0.04	**3w**	19.8 ± 1.2	>50
3c	98.0 ± 2.2	0.8 ± 0.02	**3x**	21.3 ± 0.4	>50
3d	9.7 ± 0.9	>50	**3y**	15.8 ± 0.9	>50
3e	45.2 ± 3.7	>50	**3z**	35.5 ± 0.7	>50
3f	37.4 ± 2.3	>50	**3aa**	22.0 ± 1.1	>50
3g	11.1 ± 1.1	>50	**3bb**	47.8 ± 1.6	>50
3h	44.8 ± 0.8	>50	**3cc**	39.4 ± 1.0	>50
3i	49.7 ± 1.9	>50	**3dd**	48.3 ± 0.9	>50
3j	41.0 ± 1.2	>50	**3ee**	40.3 ± 0.4	>50
3k	43.5 ± 2.1	>50	**3ff**	29.4 ± 0.8	>50
3l	36.7 ± 0.6	>50	**3gg**	38.5 ± 1.4	>50
3m	30.6 ± 1.4	>50	**3hh**	22.1 ± 0.6	>50
3n	41.8 ± 0.7	>50	**3ii**	26.6 ± 0.7	>50
3o	53.2 ± 1.8	>50	**3jj**	50.4 ± 1.6	>50
3p	48.4 ± 1.3	>50	**3kk**	24.4 ± 0.8	>50
3q	45.9 ± 0.5	>50	**3ll**	70.4 ± 1.9	26.5 ± 1.4
3r	35.3 ± 0.6	>50	*trans*-Resveratrol	67.8 ± 2.0	25.0 ± 0.8
3s	32.9 ± 1.1	>50	*cis*-Resveratrol	44.6 ± 1.7	>50
3t	21.6 ± 0.7	>50	Dihydroresveratrol	37.8 ± 0.8	>50
3u	16.6 ± 0.3	>50			

[a] The inhibition percentage was tested at a concentration of 50 μM of each compound.
[b] The IC_{50} values (μM) are the concentrations that cause 50% inhibition of aromatase.

ortho-substituted derivatives such as the trifluoromethyl and iodo derivatives **3t** and **3cc** had lower activity. The size and the electronic properties of the *meta* substituents also have a large impact on the QR1 induction ratio. The smaller and the more electronegative the substituent, the higher the IR, as could be observed for the 3-fluoro derivative **3n** (IR = 8.4). As the size of the *meta* substitu-

Table 2
Induction of QR1 by thiadiazole **3** derivatives

Compound	Hepa 1c1c7 cells			Tao c1 cells			BP^{r}c1 cells		
	IR[a,b]	CD[c,d] (μM)	% Survival[b]	IR[a,b]	CD[c,d] (μM)	% Survival[b]	IR[a,b]	CD[c,d] (μM)	% Survival[b]
3a	8.63 ± 0.21	2.1 ± 0.24	50.28	2.2	18.6	85.9	2.0	49.7	77.8
3b	2.70 ± 0.09	53.1 ± 1.3	73.5	0.6		71.6	0.5		87.8
3c	1.00 ± 0.13	>50	86.60	NT[e]			NT[e]		
3d	3.60 ± 0.18	4.0 ± 0.36	78.26	1		77.8	0.7		79.3
3e	3.00 ± 0.07	2.07 ± 0.17	96.26	1.1		83	0.6		86.4
3f	2.20 ± 0.05	16.0 ± 0.89	86.95	1.1		80.1	0.9		60.3
3g	1.20 ± 0.20	>50	94.24	NT[e]			NT[e]		
3h	7.00 ± 0.14	1.73 ± 0.24	72.55	1.6		99.1	0.5		100.0
3i	7.40 ± 0.03	1.72 ± 0.09	75.23	2.0	44.3	100.0	2.8	34.6	83.8
3j	2.00 ± 0.12	53.3 ± 1.4	97.91	1.2		91.0	0.8		71.0
3k	3.00 ± 0.22	27.7 ± 1.8	47.5	1.1		74.1	0.7		85.1
3l	1.30 ± 0.08	>50	104.7	NT[e]			NT[e]		
3m	4.40 ± 0.04	3.10 ± 0.42	102.9	1.2		73.6	1		77.3
3n	8.40 ± 0.16	4.90 ± 0.22	77.62	1.4		77.1	0.9		73.5
3o	10.50 ± 0.25	1.80 ± 0.36	86.2	1		82.5	1.7		88.4
3p	7.30 ± 0.23	0.059 ± 0.002	79.27	5.4	2.5	77.7	3.4	6.5	92.3
3q	5.10 ± 0.18	2.00 ± 0.14	47.05	1.4		74.5	1.7		56.3
3r	4.90 ± 0.07	0.44 ± 0.08	77.3	6.3	3.8	71.0	5.6	2.8	94.7
3s	4.80 ± 0.24	4.00 ± 0.16	33.71	0.8		94.9	0.6		100.4
3t	0.70 ± 0.06	2.10 ± 0.11	88.78	0.8		89.8	0.7		81.0
3u	4.20 ± 0.10	18.20 ± 0.74	88.13	2.2	41	82.8	2.4	44.5	94.7
3v	1.50 ± 0.13	>50	80.03	NT[e]			NT[e]		
3w	2.10 ± 0.09	4.00 ± 0.25	96.02	2.0	48.7	68.0	2.2	38.2	100.2
3x	0.80 ± 0.06	>50	96.81	NT[e]			NT[e]		
3y	1.00 ± 0.12	16.00 ± 0.41	88.78	0.9		96.9	0.9		98.1
3z	0.80 ± 0.14	>50	99.97	NT[e]			NT[e]		
3aa	3.80 ± 0.16	0.470 ± 0.04	37.93	7.1	2	80.2	5.7	4.4	91.5
3bb	2.30 ± 0.24	0.570 ± 0.06	71.35	1.7		68.6	1.2		95.9
3cc	2.30 ± 0.17	0.540 ± 0.03	48.77	4.0	6.3	69.8	3.9	8.1	95.1
3dd	1.50 ± 0.15	>50	49.63	NT[e]			NT[e]		
3ee	4.50 ± 0.21	5.23 ± 0.22	30.65	1.2		82.4	1.4		89.8
3ff	1.30 ± 0.11	>50	78.93	NT[e]			NT[e]		
3gg	1.80 ± 0.19	>50	46.20	NT[e]			NT[e]		
3hh	1.60 ± 0.07	>50	57.9	NT[e]			NT[e]		
3ii	6.30 ± 0.36	4.03 ± 0.31	63.7	0.6		76.3	0.8		97.1
3jj	0.70 ± 0.13	>50	36.45	NT[e]					
3kk	0.1	0.98 ± 0.07	4.0	1.2		63.7	1.4		94.3
3ll	0.70 ± 0.04	>50	66.13	NT[e]					
trans-Resveratrol	2.40 ± 0.12	21.00 ± 0.84	88.7	0.7		86.3	1.1		86.3
cis-Resveratrol	1.90 ± 0.14	>50	89.3	0.8		100.0	2.0	49.7	77.8
Dihydro-resveratrol	1.80 ± 0.21	>50	82.6	NT[e]			NT[e]		

[a] IR, induction ratio.
[b] Testing concentration, 50 μM.
[c] CD is the concentration that doubles the activity.
[d] CD values were determined for compounds with induction ratios > 2.
[e] NT, not tested.

ents became larger and the electronegativity decreased, the IR decreased too, as seen in the case of the 3-bromo **3p** and 3-iodo **3m** analogues with IR values of 7.3 and 4.4, respectively. Thiadiazoles with more polar and larger *meta* substituents such as the 3-nitrile analogue **3hh** had much lower induction ratios. Replacement of the fluoride in the *meta* position with methyl or methoxy led to lower IR values as seen in the 3-tolyl and 3-methoxy analogues **3s** and **3ii**. The *para*-substituted diphenyl thiadiazoles had weak or moderate IR values regardless the nature of the substituents as seen in the cases of **3d–g**, **3j–l**, **3z**, **3ff** and **3gg**. Furthermore, adding a *para* substituent to the *ortho*-substituted active thiadiazoles such as **3h** and **3i** afforded **3dd** and **3ee** and the IR values dropped from 7.0 and 7.4 to 1.5 and 4.5, respectively. In terms of selectivity, the most potent QR1 inducer **3o** has high QR1 selectivity since it has very low activities when tested versus the other chemopreventive targets. In terms of the concentrations of the compounds required to double the QR1 activity (CD values), many compounds showed QR1 induction activities in the sub-micromolar range, such as **3r** (CD 0.44 μM), **3aa** (CD 0.47 μM), **3bb** (CD 0.57 μM) and **3cc** (CD 0.54 μM) as shown in Table 2.

Phase II enzymes may be induced by the xenobiotic responsive element (XRE) along with phase I enzymes, or through activation of the antioxidant responsive element (ARE) without accompanying induction of phase I enzymes. Inducers which act through the XRE are said to be bifunctional; those activating ARE are monofunctional. A QR1 assay in mutant Hepa cells was used (Table 2) to determine whether the observed induction is monofunctional or bifunctional. TAOc1 and BP^{r}c1 mutant cells are defective in a functional *Ah* receptor or unable to translocate the receptor–ligand complex to the nucleus, respectively. Induction of QR1 seen in these two cell lines indicates that the sample does not work through the XRE pathway.[35]

Based on a QR1 assay in two mutant cell lines TAOc1 and BP^{r}c1 (Table 2), eight compounds were found to be monofunctional inducers of phase II enzymes. Inducers that are monofunctional are typically preferred, since they do not induce potentially toxic phase I enzymes. However, it should be noted that some quite potent bifunctional inducers, such as 4′-bromoflavone, have been found to significantly induce QR1, glutathione *S*-transferase, glutathione peroxidase, and other phase II enzymes without cytotoxic effects.[36]

Among the substituted **3a** derivatives, the hydrophobic thiadiazoles with *meta*-substituted phenyl rings exhibited potent NF-κB inhibitory activity in the sub-micromolar range (Table 3). The 3-methylphenyl thiadiazole derivative **3s** (IC_{50} 0.8 μM) was

Table 3
Evaluation of NF-κB inhibition, antioxidant, antiproliferative, and anti-inflammatory potentials of thiadiazole **3** derivatives

Compounds	NF-κB-luciferase		DPPH assay		SRB assay (MCF-7)	Nitrite assay	
	Lucif. act. % inhib[a,b]	IC_{50}[c] (μM)	% Inhibition[d]	IC_{50}[c] (μM)	IC_{50}[c] (μM)	% Inhibition[e]	IC_{50}[c] (μM)
3a	82.4 ± 5.8	47.4	8.26 ± 3.48		24.4 ± 3.3	55.7 ± 6.5	
3b	30.9 ± 8.6		−16.1 ± 1.1			1.3 ± 2.6	
3c	7.2 ± 7.0		−2.9 ± 3.2			0.9 ± 3.3	
3d	0.00		2.7 ± 6.3			5.1 ± 1.3	
3e	0.00		6.9 ± 4.4		18.8 ± 1.7	22.2 ± 2.5	
3f	0.00		0.8 ± 4.9			17.1 ± 1.7	
3g	21.2 ± 4.3		3.1 ± 5.5		17.4 ± 2.1	1.7 ± 4.4	
3h	0.00		1.8 ± 7.3		35.0 ± 2.5	9.1 ± 2.2	
3i	25.3 ± 9.6		2.8 ± 5.3		35.8 ± 4.3	−5.9 ± 5.0	
3j	0.00		2.5 ± 5.5			8.5 ± 0.7	
3k	0.00		2.9 ± 4.6			0.5 ± 4.4	
3l	0.00		16.2 ± 1.4			20.3 ± 3.3	
3m	0.00		14.3 ± 0.4		37.1 ± 3.6	15.6 ± 4.7	
3n	15.4 ± 12.0		1.3 ± 1.4		34.5 ± 2.4	3.2 ± 2.3	
3o	28.3 ± 4.1		3.8 ± 3.0		31.4 ± 3.0	24.6 ± 1.9	
3p	0.00		1.0 ± 0.5		31.0 ± 6.0	22.8 ± 2.3	
3q	0.00		11.1 ± 3.1		10.2 ± 2.5	21.4 ± 4.5	
3r	0.00		3.7 ± 1.1		39.5 ± 0.07	10.1 ± 3.0	
3s	84.4 ± 2.9	0.8	1.9 ± 1.1		22.1 ± 7.1	0.9 ± 2.2	
3t	0.00		2.9 ± 2.9			6.7 ± 2.4	
3u	40.3 ± 2.8		1.0 ± 1.7		17.8 ± 5.6	17.9 ± 4.2	
3v	38.3 ± 5.3		9.6 ± 1.4		23.5 ± 3.2	21.5 ± 5.0	
3w	20.3 ± 12.1		2.3 ± 0.5		30.3 ± 5.7	24.5 ± 0.8	
3x	35.4 ± 6.1		7.2 ± 2.6			9.6 ± 2.9	
3y	48.5 ± 5.9		1.1 ± 0.7			0.5 ± 3.7	
3z	39.4 ± 11.2		2.1 ± 0.2			−3.5 ± 5.6	
3aa	29.7 ± 5.5		1.3 ± 2.3		29.0 ± 2.8	25.9 ± 5.6	
3bb	6.7 ± 8.3		2.2 ± 0.1		39.8 ± 0.2	23.3 ± 6.8	
3cc	10.9 ± 8.3		3.4 ± 1.0			29.0 ± 2.7	30.0 ± 0.1
3dd	0.00		3.4 ± 0.4			25.0 ± 3.3	
3ee	45.8 ± 6.6		2.9 ± 0.2			25.0 ± 2.5	
3ff	15.9 ± 2.8		7.3 ± 3.3			1.6 ± 2.9	
3gg	18.2 ± 6.9		6.0 ± 2.3		31.3 ± 4.1	−0.4 ± 7.2	
3hh	46.5 ± 15.3		1.4 ± 1.3			26.4 ± 3.5	
3ii	93.9 ± 1.8	0.4 ± 0.2	−2.1 ± 3.1		24.2 ± 1.6	17.6 ± 3.1	
3jj	78.9 ± 2.8	19.3 ± 4.4	3.4 ± 5.9		4.7 ± 0.7	93.7 ± 0.5	13.50 ± 2.22
3kk	60.4 ± 9.3	38.1 ± 6.7	NT[f]			47.4 ± 13.2	
3ll	90.6 ± 8.0	7.6 ± 2.1	33.1 ± 2.4		30.8 ± 3.3	69.6 ± 3.4	23.27 ± 2.42
trans-Resveratrol	79.0 ± 6.3	0.98 ± 0.2	65.3 ± 2.3	251.1 ± 7.6		87.6 ± 0.7	30.71 ± 1.96
cis-Resveratrol	38.0 ± 8.3		33.9 ± 1.8			31.5 ± 3.1	
Dihydro-resveratrol	16.7 ± 2.4		14.7 ± 1.3		30.3 ± 3.5	36.2 ± 4.4	

[a] Testing concentration, 50 μM.
[b] NF-κB IC_{50} calculated when inhibition > 60%.
[c] The IC_{50} values are the concentrations corresponding to 50% inhibition.
[d] The inhibition percentage was tested at a concentration of 400 μM of each compound.
[e] The inhibition percentage was tested at a concentration of 40 μM of each compound.
[f] Not tested.

found to be slightly more potent than *trans*-resveratrol, while its methoxy analogues **3ii** (IC_{50} 0.4 μM) is a more potent NF-κB inhibitor. Both **3s** and **3ii** retained some QR1 induction activity (IRs 4.8 and 6.3, respectively). The more polar 3-hydroxy derivative **3kk** (IC_{50} 38 μM) is less potent than its methoxy analogue **3ii**; however, it is still more active than the unsubstituted analogue **3a**. Unlike the *meta*-methyl or -methoxy derivatives, their *para* analogues **3g** and **3x** are weakly active. Finally, the *para* amino and hydroxyl derivatives showed moderate NF-κB IC_{50} values, that is, **3jj** (IC_{50} 19 μM) and **3ll** (IC_{50} 7.6 μM).

Free radicals can cause oxidative damage to DNA, proteins, carbohydrates and lipids, with high chemical reactivity, and consequently lead to various diseases including cancer. To evaluate the antioxidant capacity, 1,1-diphenyl-2-picrylhydrazyl (DPPH) free-radical scavenging was performed according to the method of Lee et al. as described in the experimental section. In general, all of the compounds had weak or no antioxidant properties. The only compound that showed some antioxidant activity was the 4-amino derivative **3ll** (Table 3).

In normal physiology, a large amount of NO is produced by iNOS as an inflammatory mediator in host the immune system. However, NO, as one of reactive nitrogen species, can damage DNA and form nitrative (8-nitroguanine) or oxidative DNA (8-oxodG) species that eventually result in carcinogenesis.[37] In view of this, the inhibitory activities of the compounds on NO production were evaluated using the RAW 264.7 cell line-based assay to determine anti-inflammatory and cancer chemopreventive capacity. As a result, **3jj** and **3ll**, which have hydroxyl or amino groups in the *para*-position, showed better inhibition than the reference compound (*trans*-resveratrol) with IC_{50} values of 13.5 and 23.3 μM, respectively. It is noteworthy that these are the only compounds that have hydrogen-bond donor moieties in the *para*-position, suggesting that a hydrogen bond in this position might play an important role in inhibition of NO production.

Lastly, the antiproliferative potentials of the newly synthesized thiadiazoles and the reference compounds were tested with cultured MCF-7 breast cancer cells and the results are summarized in Table 3. Except for the moderately cytotoxic 4-hydroxy

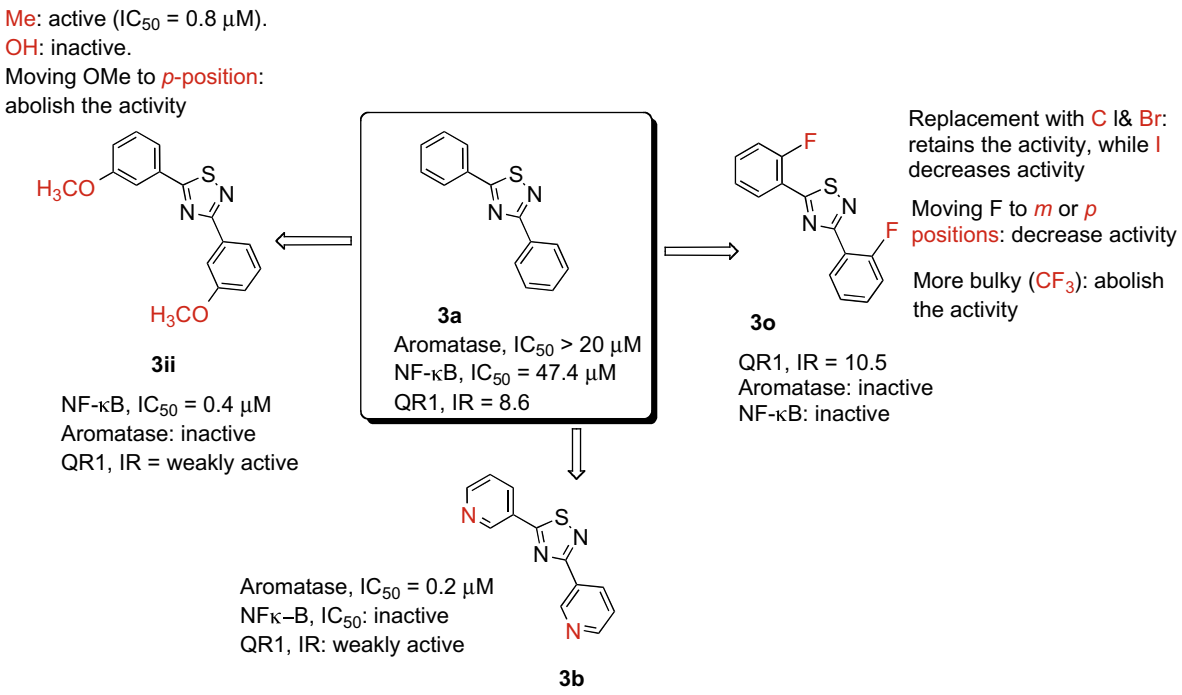

Figure 4. Summary of the chemopreventive activities of 3,5-diaryl-1,2,4-thiadiazoles.

derivative **3jj** (IC_{50} 4.7 μM), all of the compounds had weak antiproliferative activities.

3. Conclusion

The attempted optimization of the relatively weak activities of resveratrol against its many biological targets led to the 3,5-diaryl-1,2,4-thiadiazole scaffold, which provided a means to increase both potency and selectivity in aromatase and NF-κB inhibition assays, as well as in a QR1 induction assay as summarized in Figure 4. The pyridyl derivatives **3b** and **3c** had 30–125 times higher aromatase inhibitory activity (IC_{50} values of 0.2 and 0.8 μM, respectively) than *trans*-resveratrol, in addition to the advantage of the higher degree of target selectivity. *ortho*-Halo substituted derivatives **3h**, **3i**, and **3o** had very high QR1 induction ratios (IR values 7.0, 7.4, and 10.5, respectively) with a very high degree of selectivity. It is noteworthy that these IR values ranked among or even above those of the best known QR1 inducers. Finally, the *meta*-methyl or methoxy substituted derivatives **3s** and **3ii** showed equivalent or onefold more NF-κB inhibitory activity (IC_{50} values 0.8 and 0.4 μM, respectively) than *trans*-resveratrol. However, both **3s** and **3ii** are more selective than *trans*-resveratrol towards NF-κB, but they still have QR1 induction properties.

4. Experimental section

4.1. General

The integrated intensity of the major peak was ⩾95% of the combined intensities of all peaks in the HPLC traces of all biologically tested compounds. ^{1}H NMR spectra were run at 300 MHz and ^{13}C NMR spectra were run at 75.46 MHz in deuterated chloroform ($CDCl_3$) or dimethyl sulfoxide (DMSO-d_6). Chemical shifts are given in parts per million (ppm) on the delta (δ) scale. Chemical shifts are related to that of the solvent. Mass spectra were recorded at 70 eV. Melting points were determined using capillary tubes with a Mel-Temp apparatus and are uncorrected. HPLC analyses were performed using a 5 μM C-18 reverse phase column; the default setting was used (λ 254).

4.2. Preparation of thioamides 2. General procedure

Amides (1 mmol) and Lawesson's reagent (490 mg, 1.2 mmol) were added to dry THF (15 mL). The reaction mixture was stirred at room temperature for 1 h, or heated under reflux for 5 h in the case of the 4-nitro derivative. The solvent was evaporated under reduced pressure and the residue was partitioned between aq $NaHCO_3$ (25 mL) and ethyl acetate (25 mL). The organic solvent was separated and dried over anhydrous $MgSO_4$. The crude product was further purified by silica gel flash chromatography, using hexane–ethyl acetate (4:1), to yield the corresponding thioamides as yellow solids (42–60%). 4-Nitrothioamide (**2ff**),[38] 4-cyanothiobenzamide (**2gg**)[39] and 3-cyanothiobenzamide (**2hh**),[40] 3-methoxythiobenzamide (**2ii**)[41] have been previously reported.

4.3. Preparation of 1,2,4-thiadiazole derivatives 3a–ii

Thioamide (1 mmol) was added to a solution of methyl bromocyanoacetate (**1**, 215 mg, 1.2 mmol) in absolute methanol (5 mL) at room temperature. The reaction mixture was stirred for 15 s to 1 min. The precipitate was collected by filtration, washed with methanol–water (5 mL), and dried. In the case of oily compound **3z**, it was purified by silica gel chromatography using hexane–ethyl acetate (9:1).[42] Compounds **3a**,[43,44] **3b**,[45,46] **3c**,[47] **3d**,[48] **3e**,[49] **3f**, **3g**,[50] **3h**,[51] **3s**,[52] **3ff**,[53] **3jj**,[54] **3kk**[55] have previously been reported.

4.3.1. 3,5-Bis(2-bromophenyl)-1,2,4-thiadiazole (3h)

White solid (99%): mp 98 °C. ^{1}H NMR ($CDCl_3$) δ 8.51 (d, J = 7.8 Hz, 1H), 7.96 (t, J = 5.1 Hz, 2H), 7.85 (d, J = 7.5 Hz, 1H), 7.56 (m, 4H); ^{13}C NMR ($CDCl_3$) δ 187.01, 172.78, 138.14, 136.55, 131.12, 129.60, 128.95, 128.66; ESIMS (*m/z*, rel intensity) 399/397/395 (MH^+, 12/60/100); HRMS (ESI), *m/z* MH^+ 394.8858, calcd for $C_{14}H_8Br_2N_2S$ 394.8853; HPLC purity 99.61% (MeOH–H_2O, 95:5).

4.3.2. 3,5-Bis(4-(trifluoromethyl)phenyl)-1,2,4-thiadiazole (3j)

White solid (99%): mp 81 °C. ^{1}H NMR ($CDCl_3$) δ 8.49 (d, J = 5.1 Hz, 2H), 8.16 (d, J = 5.1 Hz, 2H), 7.80 (d, J = 5.1 Hz, 2H), 7.76 (d, J = 5.1 Hz, 2H); ^{13}C NMR ($CDCl_3$) δ 186.85, 172.54, 135.42, 133.30, 132.80, 128.55, 127.72, 126.30, 125.65, 125.63; CIMS (*m/z*, rel intensity) 374 (MH^+), 355 (MH^+–HF, 100); HRMS (ESI), *m/z* MH^+ 374.0316, calcd for $C_{10}H_8F_6N_2S$ 374.0312; HPLC purity 98.30% (MeOH–H_2O, 95:5).

4.3.3. 3,5-Bis(4-(*tert*-butyl)phenyl)-1,2,4-thiadiazole (3k)

White solid (99%): mp 91–92 °C. ^{1}H NMR ($CDCl_3$) δ 8.35 (d, J = 5.1 Hz, 2H), 7.98 (d, J = 5.1 Hz, 2H), 7.53 (m, 4H), 1.38 (s, 9H); ^{13}C NMR ($CDCl_3$) δ 187.73, 174.15, 155.37, 153.57, 130.68, 128.00, 127.20, 126.10, 125.40, 36.01, 31.15; ESIMS (*m/z*, rel intensity) 351 (MH^+, 100); HRMS (ESI), *m/z* MH^+ 351.1892, calcd for $C_{22}H_{26}N_2S$ 351.1895; HPLC purity 96.26% (MeOH–H_2O, 95:5).

4.3.4. 3,5-Bis(4-iodophenyl)-1,2,4-thiadiazole (3l)

Pale yellow solid (100%): mp 224–226 °C. ^{1}H NMR ($CDCl_3$) δ 8.10 (d, J = 5.4 Hz, 2H), 7.88 (d, J = 5.2 Hz, 2H), 7.86 (d, J = 5.4 Hz, 2H), 7.76 (d, J = 5.2 Hz, 2H); ^{13}C NMR ($CDCl_3$) δ 187.30, 173.04, 138.50, 137.89, 136.75, 132.08, 129.89, 128.76, 98.77, 97.21; CIMS *m/z* (rel intensity) 491 (MH^+, 52); HRMS (ESI), *m/z* 489.8489 MH^+, calcd for $C_{14}H_8I_2N_2S$ 489.8498; HPLC purity 96.8% (MeOH–H_2O, 95:5).

4.3.5. 3,5-Bis(3-iodophenyl)-1,2,4-thiadiazole (3m)

White solid (100%): mp 102–103 °C. ^{1}H NMR ($CDCl_3$) δ 8.74 (dd, J = 1.6, 1.8 Hz, 1H), 8.41 (dd, J = 1.6, 1.6 Hz, 1H), 8.36 (dd, J = 7.8, 1.6 Hz, 1H), 7.98 (dd, J = 7.8, 2.1 Hz, 1H), 7.90 (dd, J = 7.8, 1.2 Hz, 1H), 7.83 (dd, J = 7.8, 1.2 Hz, 1H), 7.26 (m, 2H); ^{13}C NMR ($CDCl_3$) δ 186.59, 172.14, 140.81, 139.33, 137.16, 135.94, 134.38, 132.18, 130.84, 130.38, 127.43, 126.71, 94.81, 94.37; CIMS *m/z* (rel intensity) 491 (MH^+, 52); HRMS (ESI), *m/z* 489.8501 MH^+, calcd for $C_{14}H_8I_2N_2S$ 489.8498; HPLC purity 97.20% (MeOH–H_2O, 95:5).

4.3.6. 3,5-Bis(3-fluorophenyl)-1,2,4-thiadiazole (3n)

White solid (100%): mp 112–113 °C. ^{1}H NMR ($CDCl_3$) δ 8.15 (d, J = 7.8 Hz, 1H), 8.08 (dd, J = 9, 0.9 Hz, 1H), 7.77 (s, 1H), 7.76 (d, J = 1.8 Hz, 1H), 7.50–7.45 (m, 2H), 7.26–7.17 (m, 2H); ^{13}C NMR ($CDCl_3$) δ 186.87, 172.52, 163.92, 161.95, 134.55, 132.26, 130.97, 130.26, 123.90, 123.27, 118.95, 117.42, 115.29, 114.22; CIMS *m/z* (rel intensity) 275 (MH^+, 49); HRMS (ESI), *m/z* 274.0374 M^+, calcd for $C_{14}H_8F_2N_2S$ 274.0376; HPLC purity 100% (MeOH–H_2O, 95:5).

4.3.7. 3,5-Bis(2-fluorophenyl)-1,2,4-thiadiazole (3o)

White solid (100%): mp 96–97 °C. ^{1}H NMR ($CDCl_3$) δ 8.47 (dt, J = 0.5, 7.5, 1 Hz, 1H), 8.33 (dt, J = 0.5, 7.5, 1 Hz, 1H), 7.56 (dt, J = 1.5, 8, 5.5 Hz, 1H), 7.49 (dt, J = 1.5, 8, 5.5 Hz, 1H), 7.37 (t, J = 8 Hz, 1H), 7.31 (m, 3H); ^{13}C NMR ($CDCl_3$) δ 182.03, 172.89, 163.92, 133.21, 133.14, 131.82, 131.74, 128.73, 124.97, 124.14, 116.87, 116.70, 116.02, 115.85; CIMS *m/z* (rel intensity) 275 (MH^+, 45); HRMS (ESI), *m/z* 274.0378 M^+, calcd for $C_{14}H_8F_2N_2S$ 274.0376; HPLC purity 100% (MeOH–H_2O, 95:5).

4.3.8. 3,5-Bis(3-bromophenyl)-1,2,4-thiadiazole (3p)

White solid (100%): mp 114–115 °C. ^{1}H NMR ($CDCl_3$) δ 8.53 (t, J = 1.5 Hz, 1H), 8.29 (d, J = 7.8 Hz, 1H), 8.21(t, J = 1.8 Hz, 1H), 7.93 (dt, J = 8.7, 1.6 Hz, 1H), 7.68 (dt, J = 7.8, 1.8, 1 Hz, 1H), 7.60 (dt, J = 8.7, 1.8, 1 Hz, 1H), 7.40 (d, J = 7.5 Hz, 1H), 7.35 (d, J = 7.8 Hz, 1H); ^{13}C NMR ($CDCl_3$) δ 186.26, 172.28, 134.88, 134.34, 133.40, 132.13, 131.33, 130.78, 130.26, 130.14, 126.81, 126.10, 123.38, 122.81; CIMS *m/z* (rel intensity) 399/397/395 (MH^+, 45/100/49); HRMS (ESI), *m/z* 393.8775 MH^+, calcd for $C_{14}H_8Br_2N_2S$ 393.8775; HPLC purity 100% (MeOH–H_2O, 95:5).

4.3.9. 3,5-Bis(2,3-dichlorophenyl)-1,2,4-thiadiazole (3q)

White solid (100%): mp 165–166 °C. ^{1}H NMR ($CDCl_3$) δ 8.53 (dd, J = 8.1, 1.2 Hz, 1H), 7.86 (dd, J = 7.6, 1.3 Hz, 1H), 7.66 (dd, J = 8.1, 1.3 Hz, 1H), 7.60 (dd, J = 7.8, 1.3 Hz, 1H), 7.43 (t, J = 8.1 Hz, 1H), 7.34 (t, J = 7.5 Hz, 1H); ^{13}C NMR ($CDCl_3$) δ 182.92, 169.34, 134.42, 134.29, 134.09, 132.80, 132.05, 131.70, 131.42, 130.32, 128.90, 127.99, 127.20; CIMS *m/z* (rel intensity) 379/377/375 (MH^+, 43/100/78); HRMS (EI), *m/z* 373.9009 M^+, calcd for $C_{14}H_6Cl_4N_2S$ 373.9006; HPLC purity 100% (MeOH–H_2O, 95:5).

4.3.10. 3,5-Bis(4-chloro-2-methylphenyl)-1,2,4-thiadiazole (3r)

White solid (100%): mp 73–74 °C. ^{1}H NMR ($CDCl_3$) δ 8.12 (d, J = 8.4 Hz, 1H), 8.00 (d, J = 8.4, 1.3 Hz, 1H), 7.36–7.26 (m, 4H), 2.71 (s, 3H), 2.65 (s, 3H); ^{13}C NMR ($CDCl_3$) δ 185.28, 172.58, 139.81, 138.72, 136.97, 135.44, 132.25, 131.59, 131.27, 130.92, 130.42, 128.43, 126.69, 126.00, 22.11, 21.84; CIMS *m/z* (rel intensity) 337/ 335 (MH^+, 16/51); HRMS (EI), *m/z* 334.0092 M^+, calcd for $C_{16}H_{12}Cl_2N_2S$ 334.0098; HPLC purity 100% (MeOH–H_2O, 95:5).

4.3.11. 3,5-Bis[2-(trifluoromethyl)phenyl]-1,2,4-thiadiazole (3t)

White solid (10%): mp >260 °C. ^{1}H NMR ($CDCl_3$) δ 7.94–7.79 (m, 4H), 7.73–7.59 (m, 4H); ^{13}C NMR ($CDCl_3$) δ 184.88, 171.18, 132.07, 131.94, 131.65, 130.92, 129.85, 129.39, 129.21, 128.96, 128.44, 126.91, 126.85, 126.77, 125.49, 121.87; CIMS *m/z* (rel intensity) 375 (MH^+, 13); HRMS (EI), *m/z* 374.0307 M^+, calcd for $C_{16}H_8F_6N_2S$ 374.0312; HPLC purity 100% (MeOH–H_2O, 95:5).

4.3.12. 3,5-Bis(2,5-dichlorophenyl)-1,2,4-thiadiazole (3u)

Off-white solid (100%): mp 116–117 °C. ^{1}H NMR ($CDCl_3$) δ 8.61 (d, J = 2.7 Hz, 1H), 8.08 (d, J = 2.7 Hz, 1H), 7.54–7.37 (m, 4H); ^{13}C NMR ($CDCl_3$) δ 182.04, 168.53, 133.80, 132.74, 132.11, 132.03, 131.94, 131.53, 130.84, 130.54, 130.06; APCIMS *m/z* (rel intensity) 379/377/375 (MH^+, 52/100/64); HRMS (ESI), *m/z* 374.9082 MH^+, calcd for $C_{14}H_7Cl_2N_2S$ 374.9079; HPLC purity 96.8% (MeOH–H_2O, 95:5).

4.3.13. 3,5-Bis(3,4-dichlorophenyl)-1,2,4-thiadiazole (3v)

Off-white solid (100%): mp 127–128 °C. ^{1}H NMR ($CDCl_3$) δ 8.44 (d, J = 1.8 Hz, 1H), 8.18 (dd, J = 1.8, 8.1 Hz, 1H), 8.14 (d, J = 2 Hz, 1H), 7.82 (dd, J = 2, 8.1 Hz, 1H), 7.56 (dd, J = 1.7, 8.1 Hz, 1H); ^{13}C NMR ($CDCl_3$) δ 186.01, 171.68, 136.44, 134.82, 133.90, 133.07, 132.19, 131.36, 130.78, 130.19, 129.97, 128.97, 127.34, 126.47; CIMS *m/z* (rel intensity) 379/377/375 (MH^+, 58/100/75); HRMS (CI), *m/z* 373.8999 M^+, calcd for $C_{14}H_6Cl_4N_2S$ 373.9006; HPLC purity 100% (MeOH–H_2O, 95:5).

4.3.14. 3,5-Bis(3-chloro-2-methylphenyl)-1,2,4-thiadiazole (3w)

Off-white solid (100%): mp 82–83 °C. ^{1}H NMR ($CDCl_3$) δ 7.90 (d, J = 6 Hz, 1H), 7.88 (d, J = 6 Hz, 1H), 7.54 (d, J = 6 Hz, 1H), 7.48 (d, J = 6 Hz, 1H), 7.28 (q, J = 6, 8.7 Hz, 2H), 2.697 (s, 3H), 2.691(s, 3H); ^{13}C NMR ($CDCl_3$) δ 186.53, 171.91, 136.41, 135.77, 134.36, 131.88, 130.74, 129.50, 128.65, 127.07, 126.55, 18.01, 17.87; CIMS *m/z* (rel intensity) 337/335 (MH^+, 71/100); HRMS (EI), *m/z* 334.0092 M^+, calcd for $C_{16}H_{12}Cl_2N_2S$ 334.0098; HPLC purity 100% (MeOH–H_2O, 95:5).

4.3.15. 3,5-Di-*p*-tolyl-1,2,4-thiadiazole (3x)

White solid (100%): mp 124–125 °C. ^{1}H NMR ($CDCl_3$) δ 8.30 (d, J = 8.4 Hz, 2H), 7.92 (d, J = 8.1 Hz, 2H), 7.31 (d, J = 8.4 Hz, 2H), 7.29 (d, J = 8.1 Hz, 2H), 2.43 (s, 3H), 2.41 (s, 3H); ^{13}C NMR ($CDCl_3$) δ 187.89, 173.73, 142.39, 140.41, 130.34, 129.85, 129.36, 128.27, 128.06, 127.36, 21.62, 21.52; ESIMS *m/z* (rel intensity) 267 (MH^+, 100); HRMS (ESI), *m/z* 267.0956 MH^+, calcd for $C_{16}H_{15}N_2S$ 267.2950; HPLC purity 99.62% (MeOH–H_2O, 95:5).

4.3.16. 3,5-Di(naphthalen-2-yl)-1,2,4-thiadiazole (3y)

White solid (100%): mp 120–121 °C. ^{1}H NMR ($CDCl_3$) δ 8.98 (s, 1H), 8.61 (s, 1H), 8.50 (dd, J = 1.5, 7.5 Hz, 1H), 8.12 (dd, J = 1.5, 7.5 Hz, 1H), 8.02–7.89 (m, 6H), 7.61–7.54 (m, 4H); ^{13}C NMR ($CDCl_3$) δ 188.15, 173.90, 134.96, 134.30, 133.24, 133.06, 130.23, 129.18, 128.97, 128.61, 128.43, 127.94, 127.78, 127.65, 127.10, 126.44, 125.18, 124.19; CIMS m/z (rel intensity) 339 (MH^+, 100); HRMS (CI), m/z 338.0876 M^+, calcd for $C_{22}H_{14}N_2S$ 338.0878; HPLC purity 100% (MeOH–H_2O, 95:5).

4.3.17. 3,5-Bis(4-butylphenyl)-1,2,4-thiadiazole (3z)

Colorless viscous oil (96%). ^{1}H NMR ($CDCl_3$) δ 8.29 (d, J = 8.0 Hz, 2H), 7.95 (d, J = 8.0 Hz, 2H), 7.32 (d, J = 8.0 Hz, 2H), 7.31 (d, J = 8.0 Hz, 2H), 2.69 (t, J = 7.5 Hz, 4H), 1.66 (q, J = 7.5 Hz, 4H), 1.63 (q, J = 7.5 Hz, 4H), 0.96 (t, J = 7.5 Hz, 6H); ^{13}C NMR ($CDCl_3$) δ 187.91, 173.78, 147.38, 145.40, 130.49, 129.23, 128.70, 128.24, 127.40, 35.65, 35.58, 33.40, 33.29, 29.66, 22.28, 13.90; ESIMS m/z (rel intensity) 373 (MNa^+, 100), 351 (MH^+, 98); HRMS (ESI), m/z 351.1901 MH^+, calcd for $C_{12}H_{27}N_2S$ 351.1889; HPLC purity 96.59% (MeOH–H_2O, 95:5).

4.3.18. 3,5-Bis(5-chloro-2-methylphenyl)-1,2,4-thiadiazole (3aa)

Off-white solid (100%): mp 80–81 °C. ^{1}H NMR ($CDCl_3$) δ 8.18 (d, J = 0.9 Hz, 1H), 8.10 (d, J = 0.9 Hz, 1H), 7.38 (dd, J = 2.1, 7.8 Hz, 1H), 7.29 (dd, J = 0.9, 7.8 Hz, 1H), 7.26 (dd, J = 0.9, 7.5 Hz, 1H), 2.69 (s, 3H), 2.64 (s, 3H); ^{13}C NMR ($CDCl_3$) δ 185.08, 172.31, 136.42, 135.38, 133.27, 133.06, 132.83, 132.30, 131.53, 131.33, 130.94, 130.69, 129.70, 129.23, 21.68, 21.52; CIMS m/z (rel intensity) 337/335 (MH^+, 66/100); HRMS (CI), m/z 334.0096 M^+, calcd for $C_{16}H_{12}Cl_2N_2S$ 334.0098; HPLC purity100% (MeOH–H_2O, 95:5).

4.3.19. 3,5-Bis(4-bromo-2-methylphenyl)-1,2,4-thiadiazole (3bb)

Off-white solid (100%): mp 74 °C. ^{1}H NMR ($CDCl_3$) δ 8.17 (d, J = 2.1 Hz, 1H), 8.10 (d, J = 2.1 Hz, 1H), 7.40 (dd, J = 2.1, 7.5 Hz, 1H), 7.33–7.25 (m, 4H), 2.69 (s, 3H), 2.65 (s, 3H); ^{13}C NMR ($CDCl_3$) δ 185.07, 172.29, 136.36, 135.34, 133.24, 133.01, 132.78, 132.25, 131.48, 131.29, 130.90, 130.64, 129.66, 129.20, 21.60, 21.46; CIMS m/z (rel intensity) 427/425/423 (MH^+, 18/100/53); HRMS (CI), m/z 421.9090 M^+, calcd for $C_{16}H_{12}Br_2N_2S$ 421.9088; HPLC purity 100% (MeOH–H_2O, 95:5).

4.3.20. 3,5-Bis(2-iodophenyl)-1,2,4-thiadiazole (3cc)

Yellowish-white solid (100%): mp 112 °C. ^{1}H NMR ($CDCl_3$) δ 8.34 (d, J = 6.9 Hz, 1H), 8.18 (d, J = 7.8 Hz, 1H), 8.08 (d, J = 7.8 Hz, 1H), 7.84 (d, J = 6.9 Hz, 1H), 7.63 (t, J = 7.8 Hz, 1H), 7.56 (d, J = 7.2 Hz, 1H), 7.34 (dt, J = 2.4, 7.5 Hz, 1H), 7.28 (dt, J = 2.4, 7.8 Hz, 1H); ^{13}C NMR ($CDCl_3$) δ 186.69, 172.17, 141.17, 140.74, 137.57, 135.78, 132.07, 131.79, 131.51, 130.92, 128.55, 128.10, 97.19, 95.59; CIMS m/z (rel intensity) 491 (MH^+, 100); HRMS (CI), m/z 489.8501 M^+, calcd for $C_{14}H_8I_2N_2S$ 489.8498; HPLC purity 100% (MeOH–H_2O, 95:5).

4.3.21. 3,5-Bis(2-bromo-4-methylphenyl)-1,2,4-thiadiazole (3dd)

Off-white solid (100%): mp 73 °C. ^{1}H NMR ($CDCl_3$) δ 8.49 (d, J = 8.4 Hz, 1H), 7.86 (d, J = 8.4 Hz, 1H), 7.58 (s, 2H), 7.29 (d, J = 8.4 Hz, 1H), 7.25 (d, J = 8.5 Hz, 1H), 2.41 (s, 3H), 2.40 (s, 3H); ^{13}C NMR ($CDCl_3$) δ 184.33, 170.50, 143.14, 141.35, 134.55, 134.27, 131.97, 131.14, 128.99, 128.84, 128.15, 123.25, 121.77, 21.05, 20.96; CIMS m/z (rel intensity) 427/425/423 (MH^+, 18/100/51); HRMS (CI), m/z 421.9090 M^+, calcd for $C_{16}H_{12}Br_2N_2S$ 421.9087; HPLC purity 95.01% (MeOH–H_2O, 95:5).

4.3.22. 3,5-Bis(2,4-dichlorophenyl)-1,2,4-thiadiazole (3ee)

White solid (100%): mp 80–81 °C. ^{1}H NMR ($CDCl_3$) δ 8.56 (d, J = 5.7 Hz, 1H), 8.03 (d, J = 8.4 Hz, 1H), 7.61 (d, J = 2.1 Hz, 1H), 7.58 (d, J = 2.1 Hz, 1H), 7.46 (dd, J = 2.1, 8.4 Hz, 1H), 7.39 (dd, J = 2.1, 8.4 Hz, 1H); ^{13}C NMR ($CDCl_3$) δ 185.47, 168.82, 137.91, 136.27, 134.33, 134.05, 133.07, 131.36, 130.77, 130.20, 128.06, 127.17; APCIMS m/z (rel intensity) 381/379/377/375 (MH^+, 12/41/100/66); HRMS (CI), m/z 374.9082 MH^+, calcd for $C_{14}H_7Cl_4N_2S$ 374.9084; HPLC purity 98.28% (MeOH–H_2O, 95:5).

4.3.23. 4,4′-(1,2,4-Thiadiazole-3,5-diyl)dibenzonitrile (3gg)

White solid (100%): mp >260 °C. IR (KBr) 3096, 2923, 2230, 1607, 1466 cm^{-1}; ^{1}H NMR ($CDCl_3$) δ 8.50 (d, J = 8.7 Hz, 2H), 8.17 (d, J = 8.5 Hz, 2H), 7.86 (d, J = 8.5 Hz, 2H), 7.82 (d, J = 8.7 Hz, 2H); ^{13}C NMR ($CDCl_3$) δ 186.61, 172.27, 136.01, 133.82, 133.15, 132.61, 128.84, 127.97, 118.41, 117.78, 115.56, 114.05; CIMS m/z (rel intensity) 289 (MH^+, 100); HRMS (CI), m/z 288.0474 M^+, calcd for $C_{16}H_8N_4S$ 288.0470; HPLC purity 98.44% (MeOH–H_2O, 95:5).

4.3.24. 3,3′-(1,2,4-Thiadiazole-3,5-diyl)dibenzonitrile (3hh)

White solid (100%): mp 176–177 °C. ^{1}H NMR ($CDCl_3$) δ 8.70 (s, 1H), 8.62 (d, J = 8.4 Hz, 1H), 8.37 (s, 1H), 8.26 (d, J = 8.1 Hz, 1H), 7.82 (d, J = 8.4 Hz, 1H), 7.78 (d, J = 8.1 Hz, 1H), 7.69–7.64 (m, 2H); ^{13}C NMR ($CDCl_3$) δ 186.32, 171.78, 135.11, 133.76, 133.38, 132.30, 132.01, 131.44, 130.77, 130.37, 129.71, 118.27, 117.54, 114.00, 113.15; CIMS m/z (rel intensity) 289 (MH^+, 100); HRMS (CI), m/z 288.0476 M^+, calcd for $C_{16}H_8N_4S$ 288.0470; HPLC purity 95.01% (MeOH–H_2O, 95:5).

4.3.25. 3,5-Bis(3-methoxyphenyl)-1,2,4-thiadiazole (3ii)

Pale yellow solid (148 mg, 100%): mp 71 °C. ^{1}H NMR ($CDCl_3$) δ 7.99 (d, J = 7.8 Hz, 1H), 7.92 (t, J = 2.1, 3.3 Hz, 1H), 7.55 (m, 2H), 7.38 (m, 2H), 7.02 (m, 2H); ^{13}C NMR ($CDCl_3$) δ 187.86, 173.44, 160.04, 159.79, 134.04, 131.69, 130.26, 129.69, 120.90, 120.00, 117.84, 116.65, 112.96, 112.05, 55.42, 55.34; CIMS m/z (rel intensity) 299 (MH^+, 100); HRMS (ESI), m/z 298.0781 M^+, calcd for $C_{16}H_{14}N_2O_2S$ 298.0776; HPLC purity 97.91% (MeOH–H_2O, 95:5).

4.3.26. 3,5-Bis(4-aminophenyl)-1,2,4-thiadiazole (3ll)

Orange-yellow solid (40%): mp 208–209 °C. ^{1}H NMR (CD_3COCD_3) δ 8.07 (d, J = 8.7 Hz, 2H), 7.79 (d, J = 8.7 Hz, 2H), 6.78 (d, J = 8.7 Hz, 2H), 6.74 (d, J = 8.7 Hz, 2H), 5.52 (br s, 2H), 5.15 (br s, 2H); ^{13}C NMR (CD_3COCD_3) δ 188.17, 174.30, 153.12, 151.28, 130.15, 129.57, 122.75, 119.72, 114.55, 114.33; CIMS m/z (rel intensity) 269 (MH^+, 100); HRMS (CI), m/z 268.0789 M^+, calcd for $C_{14}H_{12}N_4S$ 268.0783; HPLC purity 98.99% (MeOH–H_2O, 80:20).

4.4. Molecular modeling

Compounds of interest were built with Sybyl 7.1 software and minimized to 0.01 kcal/mol by the Powell method, using Gasteiger–Hückel charges and the Tripos force field. The energy-optimized compounds were docked into the androgen binding pocket of aromatase after removal of the structure of the natural ligand. The parameters were set as the default values for GOLD. The maximum distance between hydrogen bond donors and acceptors for hydrogen bonding was set to 3.5 Å. After docking, the first pose conformations of compounds of interest were merged into the ligand–free protein. The new ligand–protein complex was subsequently subjected to energy minimization using the Amber force field with Amber charges. During the energy minimization, the structure of the compounds of interest and a surrounding 10 Å sphere of the protein were allowed to move. The structure of remaining protein was kept frozen. The energy minimization was performed using the Powell method with a 0.05 kcal/(mol Å)

energy gradient convergence criterion and a distance dependent dielectric function.

4.5. Aromatase assay

Aromatase activity was assayed as previously reported, with the necessary modifications to assay in a 384-well plate.[56] Briefly, the test compound (3.5 μL) was preincubated with 30 μL of NADPH-regenerating system (2.6 mM $NADP^+$, 7.6 mM glucose-6-phosphate, 0.8 U/mL glucose-6-phosphate dehydrogenase, 13.9 mM $MgCl_2$, and 1 mg/mL albumin in 50 mM potassium phosphate buffer, pH 7.4) for 10 min at 37 °C. As a source of aromatase we use BD-Supersomes™ a well-established source of cDNA-expressed enzymes. BD recommends using NADPH generating system for cytochrome P450 activity. An NADPH solution can also be used but depletion of this cofactor might happen during longer incubations. Before addition of the enzyme and substrate mixture (33 μL of 1 μM CYP19 enzyme, BD Biosciences, 0.4 μM dibenzylfluorescein, 4 mg/mL albumin in 50 mM potassium phosphate, pH 7.4) was added, and the plate was incubated for 30 min at 37 °C before quenching with 25 μL of 2 N NaOH. After termination of the reaction and shaking for 5 min, the plate was further incubated for 2 h at 37 °C. This enhances the ratio of signal to background. Fluorescence was measured at 485 nm (excitation) and 530 nm (emission). IC_{50} values were based on three independent experiments performed in duplicate using five concentrations of test substance. Naringenin (IC_{50} = 0.23 μM) was used as a positive control.

Kinetic aromatase assays were carried out in order to determine inhibitor mechanism. Test compound was preincubated with 30 μL of NADPH-regenerating system (2.6 mM $NADP^+$, 7.6 mM glucose 6-phosphate, 0.8 U/mL glucose 6-phosphate dehydrogenase, 13.9 mM $MgCl_2$, and 1 mg/mL albumin in 50 mM potassium phosphate buffer, pH 7.4) for 10 min at 37 °C. The IC_{50} was used as the final concentration for each inhibitor. Substrate was added at five concentrations: 16, 8, 4, 2, and 1 μM. CYP19 (1 μM) was added and fluorescence was measured at 485 nm (excitation) and 530 nm (emission) every 10 s for at least 5 min. Error values represent three independent experiments for each compound.

4.6. Quinone reductase 1 (QR1) assay

Hepa 1c1c7 (mouse hepatoma) cells, TAOc1 mutant Hepa cells, or BP^rC1 mutant Hepa cells were used in the assay. Cells were incubated in a 96-well plate with test compounds at a maximum concentration of 50 μM, digitonin was used to permeabilize cell membranes, and enzyme activity was measured by the reduction of 3-(4,5-dimethylthiazo-2-yl)-2,5-diphenyltetrazolium bromide (MTT) to a blue formazan. Production was measured by absorption at 595 nm. A total protein assay using crystal violet staining was run in parallel. 4′-Bromoflavone (CD = 0.01 μM) was used as a positive control. Mutant cell lines TAOc1 and BP^rc1 were supplied by Dr. J.P. Whitlock, Jr. (Department of Molecular Pharmacology, Stanford University School of Medicine, Stanford, California 94305, USA). All cells were maintained and passaged according to ATCC instructions in MEM-α containing 5% antibiotic–antimycotic and 10% fetal bovine serum at 37 °C in a 5% CO_2 atmosphere. The assay in these cells follows the procedure of the QR1 assay described in wild type Hepa1c1c7 cells.

4.7. NF-κB luciferase assay

Studies were performed with NF-κB reporter stably-transfected human embryonic kidney cells 293 from Panomics (Fremont, CA). This cell line contains chromosomal integration of a luciferase reporter construct regulated by NF-κB response element. The gene product, luciferase enzyme, reacts with luciferase substrate, emitting light, which is detected with a luminometer. Data were expressed as % inhibition at 50 μM or IC_{50} values (i.e., concentration of test sample required to inhibit TNF-α activated NF-κB activity by 50%). After incubating treated cells, they were lysed in Reporter Lysis buffer. The luciferase assay was performed using the Luc assay system from Promega, following the manufacturer's instructions. In this assay, *N*-α-tosyl-L-phenylalanine chloromethyl ketone (TPCK) was used as a positive control; IC_{50} = 5.09 μM.

4.8. Nitrite assay

RAW 264.7 mouse macrophage cells were incubated in a 96-well culture plate for 24 h. The cells were pretreated with various concentrations of compounds dissolved in phenol red-free DMEM for 30 min followed by 1 μg/mL of LPS treatment for 24 h. The level of nitrite, a stable end product of NO, in the cultured media was measured using a colorimetric reaction with Griess reagent. The optical density (OD) was measured at 540 nm and the level of nitrite was estimated using a standard curve with known concentrations of sodium nitrite. The positive control in this assay was N^G-L-monomethyl arginine (L-NMMA); IC_{50} = 19.7 μM. In parallel, the cytotoxic effects of compounds were evaluated by SRB assay

4.9. 2,2-Diphenyl-1-picrylhydrazyl (DPPH) free radical scavenging assay

To evaluate antioxidant capacity, 1,1-diphenyl-2-picrylhydrazyl (DPPH) free-radical scavenging was performed according to the method described by Lee et al. In this assay,[57] antioxidants convert the stable free radical DPPH to an inactive hydrazine form, accompanied by color fading from purple to pale yellow. Briefly, 95 μL of DPPH radical solution in ethanol (316 μM) was added in a 96-well plate containing 5 μL of each compound dissolved in 100% DMSO, and the mixture incubated for 30 min at 37 °C. The OD of each well was measured at 515 nm using a microplate reader. The DPPH radical scavenging activity of each sample was evaluated by calculating % inhibition as follows: % inhibition = $(1 - OD_{sample}/OD_{control}) \times 100$.

4.10. SRB assay[58]

Serially diluted test compounds in DMSO were transferred to 96-well plates and incubated for 72 h at 37 °C in a CO_2 incubator. The incubation was stopped by adding trichloroacetic acid (10%), which fixes cells. The cells were washed, air-dried, stained with 0.4% SRB solution, and optical densities were determined at 515 nm using a microplate reader. In each case, a zero-day control was performed by adding an equivalent number of cells (1×10^4 cells per well), incubating at 37 °C for 30 min, and processing as described above. Percent of cell survival was calculated using the formula: $(OD_{tested\ compound} - OD_{zero\text{-}day})/OD_{control} - OD_{zero\text{-}day}) \times 100$.

Acknowledgment

This work was supported by Program Project Grant P01 CA48112 awarded by the National Cancer Institute.

References and notes

1. Catella-Lawson, F.; Fitzgerald, G. A. *Drug Saf.* **1995**, *13*, 69–75.
2. (a) Fisher, B.; Costantino, J. P.; Wickerham, D. L.; Cecchini, R. S.; Cronin, W. M.; Robidoux, A.; Bevers, T. B.; Kavanah, M. T.; Atkins, J. N.; Margolese, R. G.; Runowicz, C. D.; James, J. M.; Ford, L. G. *J. Natl. Cancer Inst.* **1998**, *90*, 1371–1388; (b) Kramer, R.; Brown, P. *Drug Saf.* **2004**, *27*, 979–989.
3. Parnes, H. L.; Thompson, I. M.; Ford, L. G. *J. Clin. Oncol.* **2005**, *23*, 368–377.
4. Hong, W. K.; Sporn, M. B. *Science* **1997**, *278*, 1073–1077.

5. Conda-Sheridan, M.; Marler, L.; Park, E.; Kondratyuk, T. P.; Jermihov, K.; Mesecar, A. D.; Pezzuto, J. M.; Asolkar, R. N.; Fenical, W.; Cushman, M. *J. Med. Chem.* **2010**, *53*, 8688–8699.
6. Aggarwal, B. B.; Shishodia, S. *Biochem. Pharmacol.* **2006**, *71*, 1397–1421.
7. Strasser-Weippl, K.; Goss, P. E. *J. Clin. Oncol.* **2005**, *23*, 1751–1759.
8. (a) Hoshino, J.; Park, E.; Kondratyuk, T. P.; Marler, L.; Pezzuto, J. M.; van Breemen, R. B.; Mo, S.; Li, Y.; Cushman, M. *J. Med. Chem.* **2010**, *53*, 5033–5043; (b) Ghosh, S.; Choudary, A.; Musi, N.; Hu, Y. F.; Li, R. *Mol. Endocrinol.* **2009**, *23*, 662–670.
9. Aktan, F. *Life Sci.* **2004**, *75*, 639–653.
10. Aggarwal, B. B.; Gehlot, P. *Curr. Opin. Pharmacol.* **2009**, *9*, 351–369.
11. Ross, D.; Kepa, J. K.; Winski, S. L.; Beall, H. D.; Anwar, A. H. D.; Siegel, D. *Chem. Biol. Interact.* **2000**, *129*, 77–97.
12. Sheikh, M. S.; Huang, Y. *Cell Cycle* **2003**, *2*, 550–552.
13. Escárcega, R. O.; Fuentes-Alexandro, S.; García-Carrasco, M.; Gatica, A.; Zamora, A. *Clin. Oncol. (R. Coll. Radiol.)* **2007**, *19*, 154–161.
14. Hayden, M. S.; West, A. P.; Ghosh, S. *Oncogene* **2006**, *25*, 6758–6780.
15. Fitzgerald, D. C.; Meade, K. G.; McEvoy, A. N.; Lillis, L.; Murphy, E. P.; MacHugh, D. E.; Baird, A. W. *Vet. Immunol. Immunopathol.* **2007**, *116*, 59–68.
16. Chandel, N. S.; Trzyna, W. C.; McClintock, D. S.; Schumacker, P. T. *J. Immunol.* **2000**, *165*, 1013–1021.
17. Hargrave, B. Y.; Tiangco, D. A.; Lattanzio, F. A.; Beebe, S. J. *Cardiovasc. Toxicol.* **2003**, *3*, 141–151.
18. Hiscott, J.; Kwon, H.; Génin, P. *J. Clin. Invest.* **2001**, *107*, 143–151.
19. Pezzuto, J. M. *J. Agric. Food Chem.* **2008**, *56*, 6777–6784. Ref. 37 cited therein.
20. Jang, M.; Cai, L.; Udeani, G. O.; Slowing, K. V.; Thomas, C. F.; Beecher, C. W. W.; Fong, H. H. S.; Farnsworth, N. R.; Kinghorn, A. D.; Mehta, R. G.; Moon, R. C.; Mezzuto, J. M. *Science* **1997**, *275*, 218–220.
21. (a) Pizarro, J. G.; Verdaguer, E.; Ancrenaz, V.; Junyent, F.; Sureda, F.; Pallàs, M.; Folch, J.; Camins, A. *Neurochem. Res.* **2011**, *36*, 187–194; (b) Oi, N.; Jeong, C. H.; Nadas, J.; Cho, Y. Y.; Pugliese, A.; Bode, A. M.; Dong, Z. *Cancer Res.* **2010**, *70*, 9755–9764.
22. (a) Carbó, N.; Costelli, P.; Baccino, F. M.; López-Soriano, F. J.; Argilés, J. M. *Biochem Biophys. Res. Commun.* **1999**, *254*, 739–743; (b) Chen, Y.; Tseng, S. H.; Lai, H. S.; Chen, W. J. *Surgery* **2004**, *136*, 57–66; (c) Roy, P.; Kalra, N.; Prasad, S.; George, J.; Shukla, Y. *Pharm. Res.* **2009**, *26*, 211–217; (d) Aziz, M. H.; Kumar, R.; Ahmad, N. *Int. J. Oncol.* **2003**, *23*, 17–28.
23. Pezzuto, J. M. *Pharm. Biol.* **2008**, *46*, 443–573.
24. Pezzuto, J. M. *Biochem. Pharmacol.* **1997**, *53*, 121–133.
25. Ma, Z.; Molavi, O.; Haddadi, A.; Lai, R.; Gossage, R. A.; Lavasanifar, A. *Cancer Chemother. Pharmacol.* **2008**, *63*, 27–35.
26. Deng, Y. H.; Alex, D.; Huang, H. Q.; Wang, N.; Yu, N.; Wang, Y. T.; Leung, G. P.; Lee, S. M. *Phytother. Res.* **2011**, *25*, 451–457.
27. Sun, B.; Hoshino, J.; Jermihov, K.; Marler, L.; Pezzuto, J. M.; Mesecar, A. D.; Cushman, M. *Bioorg. Med. Chem.* **2010**, *18*, 5352–5366.
28. (a) Simoni, D.; Grisolia, G.; Giannini, G.; Roberti, M.; Rondanin, R.; Piccagli, L.; Baruchello, R.; Rossi, M.; Romagnoli, R.; Invidiata, F. P.; Grimaudo, S.; Jung, M. K.; Hamel, E.; Gebbia, N.; Crosta, L.; Abbadessa, V.; Di Cristina, A.; Dusonchet, L.; Meli, M.; Tolomeo, M. *J. Med. Chem.* **2005**, *48*, 723–736; (b) Romagnoli, R.; Baraldi, P. G.; Cruz-Lopez, O.; Cara, C. L.; Carrion, M. D.; Brancale, A.; Hamel, E.; Chen, L.; Bortolozzi, R.; Basso, G.; Viola, G. *J. Med. Chem.* **2010**, *53*, 4248–4258; (c) Schobert, R.; Biersack, B.; Dietrich, A.; Effenberger, K.; Knauer, S.; Mueller, T. *J. Med. Chem.* **2010**, *53*, 6595–6602.
29. Ghosh, D.; Griswold, J.; Erman, M.; Pangborn, W. *Nature* **2009**, *457*, 219–223.
30. Verdonk, M. L.; Cole, J. C.; Hartshorn, M. J.; Murray, C. W.; Taylor, R. D. *Protein: Struct., Funct., Genet.* **2003**, *52*, 609–623.
31. Ekroos, M.; Sjogren, T. *Proc. Natl. Acad. Sci. U.S.A.* **2006**, *103*, 13682–13687.
32. (a) Buzdar, A.; Douma, J.; Davidson, N.; Elledge, R.; Morgan, M.; Smith, R.; Porter, L.; Nabholtz, J.; Xiang, X.; Brady, C. *J. Clin. Oncol.* **2001**, *19*, 3357–3366; (b) Eisen, A.; Trudeau, M.; Shelley, W.; Messersmith, H.; Pritchard, K. I. *Cancer Treat. Rev.* **2008**, *34*, 157–174.
33. Ghosh, G.; Van Duyne, G.; Ghosh, S.; Sigler, P. B. *Nature* **1995**, *373*, 303–310.
34. Kennelly, E. J.; Gerhauser, C.; Song, L. L.; Graham, J. G.; Beecher, C. W. W.; Pezzuto, J. M.; Kinghorn, A. D. *J. Agric. Food Chem.* **1997**, *45*, 3771–3777.
35. Gerhäuser, C.; You, M.; Liu, J.; Moriarty, R. M.; Hawthorne, M.; Mehta, R. G.; Moon, R. C.; Pezzuto, J. M. *Cancer Res.* **1997**, *57*, 272–278.
36. Marler, L.; Conda-Sheridan, M.; Cinelli, M. A.; Morrell, A. E.; Cushman, M.; Chen, L.; Huang, K.; Van Breemen, R.; Pezzuto, J. M. *Anticancer Res.* **2010**, *30*, 4873–4882.
37. Hiraku, Y.; Kawanishi, S.; Ichinose, T.; Murata, M. *Ann. N.Y. Acad. Sci.* **2010**, *1203*, 15–22.
38. Ciureanu, M.; Hillebrand, M.; Volanschi, E.; Ghetu, D. *Rev. Roum. Chim.* **1987**, *32*, 467–475.
39. Zhu, B.; Bauer, S. M.; Jia, Z. J.; Probst, G. D.; Zhang, Y.; Scarborough, R. M. 2006, PCT Int. Appl. WO 2006002099.
40. Oda, K.; Sakai, M.; Machida, M. *Chem. Pharm. Bull.* **1997**, *45*, 584–589.
41. Michael, N.; Claudia, P.; Andrea, B.; Walther, S. *Synthesis* **2008**, *24*, 4012–4018.
42. Mayhoub, A. S.; Kiselev, E.; Cushman, M. *Tetrahedron Lett.* **2011**, *52*, 4941–4943.
43. Toland, W. G. *J. Org. Chem.* **1962**, *27*, 869–871.
44. Kresze, G.; Horn, A.; Philippson, R.; Trede, A. *Chem. Ber.* **1965**, *98*, 3401–3409.
45. Boeini, H. Z. *J. Iran. Chem. Soc.* **2009**, *6*, 547–551.
46. Yan, M.; Chen, Z.; Zheng, Q. *J. Chem. Res., Synop.* **2003**, *10*, 618–619.
47. Meltzer, R. I.; Lewis, A. D.; King, J. A. *J. Am. Chem. Soc.* **1955**, *77*, 4062–4066.
48. Kresze, G.; Mashke, A.; Albrecht, R.; Bederke, K.; Patzchke, H. P.; Smalla, H.; Trede, A. *Angew. Chem.* **1962**, *74*, 135–144.
49. Khosropour, A. R.; Noei, J. *Monatsh. Chem.* **2010**, *141*, 649–651.
50. Rafiqul-Islam, M.; Shimada, K.; Aoyagi, S.; Takikawa, Y.; Kabuto, C. *Heteroat. Chem.* **2004**, *15*, 175–186.
51. Komatsu, M.; Shibata, J.; Ohshiro, Y.; Agawa, T. *Bull. Chem. Soc. Jpn.* **1983**, *56*, 180–183.
52. Cheng, D.; Chen, Z. *Synth. Commun.* **2002**, *32*, 2155–2159.
53. Patil, P. C.; Bhalerao, D. S.; Dangate, P. S.; Akamanchi, K. G. *Tetrahedron Lett.* **2009**, *50*, 5820–5822.
54. Hartmann, R.; Frotscher, M.; Oberwinkler, S.; Bey, E. PCT Int. Appl. 2009, WO 2009027346 A2 20090305.
55. Bey, E.; Marchais-Oberwinkler, S.; Werth, R.; Negri, M.; Al-Soud, Y. A.; Kruchten, P.; Oster, A.; Frotscher, M.; Birk, B.; Hartmann, R. W. *J. Med. Chem.* **2008**, *51*, 6725–6739.
56. Maiti, A.; Cuendet, M.; Croy, V. L.; Endringer, D. C.; Pezzuto, J. M.; Cushman, M. *J. Med. Chem.* **2007**, *50*, 2799–2806.
57. Lee, S. K.; Mbwambo, Z. H.; Chung, H.; Luyengi, L.; Gamez, E. J.; Mehta, R. G.; Kinghorn, A. D.; Pezzuto, J. M. *Comb. Chem. High Throughput Screen* **1998**, *1*, 35–46.
58. You, M.; Wickramaratne, D. B.; Silva, G. L.; Chai, H.; Chagwedera, T. E.; Farnsworth, N. R.; Cordell, G. A.; Kinghorn, A. D.; Pezzuto, J. M. *J. Nat. Prod.* **1995**, *58*, 598–604.